J. Membrane Biol. 176, 53–65 (2000)
DOI: 10.1007/s00232001075

The Journal of
Membrane
Biology

Apical Na^+-Cl^- Symport in Rabbit Gallbladder Epithelium: A Thiazide-Sensitive Cotransporter (TSC)

D. Cremaschi, C. Porta, G. Bottà, C. Bazzini, M.D. Baroni, M. Garavaglia

Dipartimento di Fisiologia e Biochimica Generali, Sezione di Fisiologia Generale, Università degli Studi di Milano, Via Celoria 26, I-20133 Milan, Italy

Received: 29 July 1999/Revised: 23 March 2000

Abstract. Cl^- apically enters the epithelium of rabbit gallbladder by a Na^+-Cl^- symport, sensitive to hydrochlorothiazide (HCTZ). Since HCTZ also activates an apical SITS-sensitive Cl^- conductance (G_{Cl}), the symport inhibition might be merely due to a short circuit of the symport by G_{Cl} rather than to a direct action of HCTZ on the symporter. To examine whether the symport is directly inhibited by HCTZ and whether the symporter belongs to the family of thiazide-sensitive cotransporters (TSC), radiochemical measurements of the apical Cl^- uptake, electrophysiological determinations of intracellular Cl^- and Na^+ activities ($a_{i,Cl}$ and $a_{i,Na}$) with selective theta microelectrodes and molecular biology methods were used. The $^{36}Cl^-$ uptake proved to be a measurement of the apical unidirectional Cl^- influx (J_{mc}) and of the symport only (without backflux components), with measuring times of 45 sec under all experiment conditions; its inhibition by HCTZ was unaffected by G_{Cl} activation or abolition. After HCTZ treatment the decrease in $a_{i,Cl}$ (measured as the initial rate or in 3 min) was larger than the decrease in $a_{i,Na}$. The difference was reduced to one third in a group of epithelia in which the elicited G_{Cl} was reduced to one third; moreover it was abolished in any case when G_{Cl} was abolished with 10^{-4} M SITS. The SITS-insensitive rate of $a_{i,Cl}$ decrease was equal to that of the $a_{i,Na}$ decrease in any case. Thus the $a_{i,Cl}$ decrease displays a component dependent on G_{Cl} activation and a second component dependent on symport inhibition. Using the RT-PCR technique a cDNA fragment was obtained that was 99% identical to the corresponding region of the rabbit renal TSC isoform. The results indicate that in rabbit gallbladder epithelium HCTZ displays a dual action, namely G_{Cl} activation and Na^+-Cl^- symport inhibition. This Na^+-Cl^- symporter is the first TSC found to be functionally expressed in a nonrenal or nonrenal-like epithelium.

Key words: Hydrochlorothiazide — SITS — Intracellular Cl^- activity — Intracellular Na^+ activity — Unidirectional Cl^- influx — Cl^- conductance

Introduction

In the epithelium of rabbit gallbladder, the very large transepithelial transport of NaCl is sustained at the apical entry by two electroneutral transports: a Na^+/H^+,Cl^-/HCO_3^- double exchange and a Na^+-Cl^- symport. The double exchange is completely dependent on exogenous HCO_3^-/CO_2; it can be eliminated by inhibiting carbonic anhydrase with acetazolamide, or by avoiding HCO_3^-/CO_2 in the media and bubbling with 100% O_2. The symport is insensitive to K^+, furosemide and bumetanide: the corresponding transporter does not belong to the family of the bumetanide-sensitive cotransporters (BSC) [11–14, 26].

Conversely, this Na^+-Cl^- symport is inhibited by hydrochlorothiazide (HCTZ) [16, 26]. In fact: (i) with HCO_3^-/CO_2-free media, bubbled with 100% O_2, all apical Cl^- entry into the cell is due to the symport, [11, 12, 14] (ii) under these conditions HCTZ on the apical side abolishes the apical Cl^- uptake measured radiochemically in 45 sec [16]. Accordingly, HCTZ also reduces intracellular Cl^- activity towards the electrochemical equilibrium and inhibits transepithelial NaCl transport [16]. Although uptake inhibition starts at the beginning of treatment, it is complete within 10 to 15 min; during this latter period a new Cl^- influx, sensitive to bumetanide, is homeostatically activated [16]. The HCTZ action on the symport has also been observed on apical membrane

Correspondence to: D. Cremaschi

vesicles [26]. However, whereas no apical Cl^- conductance (G_{Cl}) is present under basal conditions [10, 12, 18, 23, 37], a substantial apical stilbene-sensitive G_{Cl} of 2.3 $\times 10^{-3}$ S cm^{-2} is elicited by HCTZ; it is detectable in a few tens of seconds and completely activated in 7–9 min [18]. The $^{36}Cl^-$ uptake through G_{Cl} is negligible, due to the large negative apical membrane potential (*see also* Materials and Methods); conversely, the cell to lumen Cl^- efflux though G_{Cl} is measurable [15]. Thus, the observed symport inhibition by thiazide might be due to a symport short circuit caused by the parallel G_{Cl} rather than to a direct HCTZ action on the symporter: the apical $^{36}Cl^-$ uptake may be reduced by a rapid return to the lumen (through the activated G_{Cl}) of the $^{36}Cl^-$ pushed into the cell by the symport. Equally, the decrease in intracellular Cl^- activity may be produced by the cell to lumen Cl^- backflux through G_{Cl} [15], with consequent inhibition of transepithelial NaCl transport.

On this basis, the aim of this study was to ascertain whether the Na^+-Cl^- symport is directly inhibited by HCTZ or simply short circuited. In the first case HCTZ would act directly on the symporter, which would then be identical or similar to that found in the distal tubule and fish urinary bladder [6, 19, 36, 38, 39] and would belong to the family of thiazide-sensitive cotransporters (TSC): the gallbladder epithelium would be the first extra-renal epithelium to show it working. In the second case the symporter found would be a new symporter, insensitive to thiazide and resistant to all the inhibitors of double ion exchangers and known cotransporters.

To examine this alternative, radiochemical methods (measurement of transapical Cl^- uptake), electrophysiological methods (determination of intracellular Cl^- and Na^+ activities with selective theta microelectrodes) and molecular biology methods were used.

Materials and Methods

Male New Zealand rabbits (body weight about 3 Kg), kept for 10 days under constant conditions of light/dark and temperature and fed with standard pellets, were killed by cervical dislocation. The excised gallbladders were washed free of bile with saline solution.

Measurements of Total Cl^- Uptake

The method used was very similar to that previously reported [16]. Briefly, gallbladders, opened flat, were mounted, carefully avoiding any stretching, on a nylon mesh between two Lucite chambers, with the luminal surface facing upwards (exposed area: 0.6 cm^2). The luminal solution (0.8 ml) was agitated by bubbling the appropriate gas mixture; conversely, the serosal chamber was continuously perfused with gassed saline moved by a peristaltic pump. After a 30-min preincubation period in Krebs-Henseleit solution, the tissue was allowed to equilibrate on both sides for 45 min in bicarbonate-free saline. Then it was washed five times on the luminal side with the test solution and finally exposed for 45 sec to the same saline, to which ^{3}H-sucrose (5 μCi/ml) and $^{36}Cl^-$ (4 μCi/ml) were added. Variations in incubation and treatment on the luminal side will be described later. At the end of the experiment the luminal medium was withdrawn, the tissue squeezed with an ice-cold isotonic solution of mannitol and punched off. It was then bathed in 2 ml of bidistilled water, frozen at −20°C, thawed, boiled for 15 min and centrifuged. Samples in triplicate of the supernatant and the incubation fluid were assayed for radioactivity by a liquid scintillation spectrometer (Minaxi-TriCarb, 4000 series Packard Instruments, Zurich). The measured influx was expressed as μmol cm^{-2} hr^{-1}.

Measurement of Apical and Paracellular Cl^- Uptake

Under control conditions the cellular fraction of the total Cl^- uptake was estimated by treating the luminal side of the tissue with 25 mM SNC^- during the 45-sec measuring time; in fact it is known that the entire apical Cl^- entry is neutrally coupled with Na^+ and completely inhibitable with SCN^-; the residual fraction is insensitive to Na^+ and SCN^- and is paracellular [7, 9, 11, 12, 14]. The opening of the apical G_{Cl} by HCTZ per se should increase the lumen to cell unidirectional flux (J_{mc}). Since G_{Cl} is partially inhibited by 25 mM SCN^- [18], in principle, under treatment conditions, not of all the SCN^- sensitive fraction of Cl^- uptake should be ascribed to the coupled neutral transport, nor should all be the SCN^--insensitive fraction paracellular. However, the new apical conductive unidirectional flux (J^G_{mc}) proves negligible compared with the unidirectional apical neutral transport and paracellular flux. In fact, knowing that the opened G_{Cl} is 2.3 $\times 10^{-3}$ S cm^{-2} at most [18], the corresponding permeability coefficient (P_{Cl}) can be calculated

$$P_{Cl} = G_{Cl} \cdot \frac{RT}{\bar{C}_{Cl} \cdot z_{Cl}^2 \cdot F^2} = 7.9 \times 10^{-6} \text{ cm sec}^{-1}$$

(symbols used with the usual meanings). Hence the apical conductive unidirectional Cl^- influx with apical membrane potential (V_m) equal to zero ($_0J^G_{mc}$) is

$$_0J^G_{mc} = P_{Cl} \cdot C_{Cl,out} = 3.6 \text{ μmol cm}^{-2} \text{ hr}^{-1}$$

and the apical conductive unidirectional Cl^- influx in the presence of the apical membrane potential measured under HCTZ treatment (J^G_{mc}) is $J^G_{mc} = {}_0J^G_{mc}\,[\exp(z_{Cl} FV_m/RT)]^{-1/2} = 1.1$ μmol cm^{-2} hr^{-1} (for the eq.: ref. 34) about half of which is SCN^--sensitive. Thus, the apical conductive SCN^--sensitive and insensitive components (about 0.5 μmol cm^{-2} hr^{-1} at most for each one) fall within the error of measurement of the SCN^--sensitive and insensitive fractions. Since G_{Cl} is generally one-third lower than the maximal value reported above, the conductive influx influence is even more negligible. The fact that the HCTZ induced conductive increase of the apical Cl^- uptake is actually negligible is emphasized by the finding that within 15 min the apical uptake is completely abolished by HCTZ (*see* Introduction). On this basis, under all conditions the SCN^--sensitive fraction of the uptake was considered apical and neutrally coupled to Na^+, whereas the SCN^--insensitive fraction was considered paracellular.

Measurements of Apical Membrane Potential and Intracellular Na^+ and Cl^- Activities

To measure intracellular ion activities, Na^+- or Cl^--theta microelectrodes (one conventional and one ion-selective channel) with tips of 0.2–0.3 μm were prepared by the method previously described [27]. The Na^+- and Cl^--sensitive resins (labeled I-ETH227 and 477913 respectively) came from Fluka AG (CH-9740 Buchs, Switzerland) and

Corning (NY) or were prepared in the laboratory on the basis of the known compositions. Pyrex theta tubings (with diameter = 1.5 mm) were purchased from World Precision Instruments (Sarasota, FL). Na^+- or Cl^--sensitive channels and their corresponding conventional channels of the microelectrode were backfilled with 154 mM NaCl or KCl and 500 or 154 mM KCl, respectively. Each electrode was calibrated in isosmotic test solutions of NaCl-KCl for the Na^+-sensitive resin, and NaCl-sodium gluconate for the Cl^--sensitive resin; the sums of the Na^+ and K^+ or Cl^- and gluconate activities were kept constant at 112.4 mM (total concentration = 154 mM). When Na^+ or Cl^- activity of the calibration solution was changed from 112.4 to 11.2 mM, the voltage of the selective channel changed by about 52 mV in both cases and that of the conventional channel (tip potential and diffusion potential together) by less than 1 mV. The resistances of the Na^+- and Cl^--sensitive channels were 30–120 and 5–10 × 10^9 Ω, respectively; after bevelling for 5 min in 40% alumina (w/v) and polishing by dipping the tip in 0.5% agar, the resistance of the Na^+-sensitive channels decreased to values comparable to those of the Cl^--sensitive channels (8–20 × 10^9 Ω). The time necessary to achieve a complete response was about 12 sec for both Cl^-- and Na^+-sensitive channels. With the Ca^{2+} activity of the phosphate-saline used, the Na^+ resin showed a small interference due to Ca^{2+}. The voltage variation introduced by the presence of Ca^{2+} in the saline was subtracted from the measured values; the difference was used to determine Na^+ activity on the calibration curve. The Cl^- resin did not demonstrate dependence on phosphate and sulfate when these anions were present at the activities of the incubation solution used or at what is presumably their cell activity. Moreover, the Cl^- resin was insensitive to 10^{-3} M HCTZ, at least for about 30 min continuous exposure; conversely, it was strongly affected by SITS, but completely protected against it when the microelectrode tip was in the cell.

The set up for potential recordings was that previously reported [16] with the exception that the short pulses of direct current (20 μA) were generated by a SD5 Stimulator-Grass Instruments (Quincy, MA). The mounted tissue separated an upper mucosal from a lower serosal Lucite chamber (window: 0.17 cm^2), both perfused (12 ml/min) by gravity and kept inclined so as to minimize fluctuations of the fluid level on the epithelium; the fluid was finally collected in a beaker and sent back to the reservoir by a peristaltic pump (Minipuls 2, Gilson, Villiers le Bel, France) so as to keep the reservoir level constant. The time required for renewal of the fluid on the epithelium was 4–5 sec.

Intracellular activities were measured with prolonged single impalements (about one per gallbladder). They were generally 7 min long with the following protocol: control (1 min), saline renewal or treatment (3 min), back to control (3 min). The microelectrode response was again checked at the end of the impalement with calibration solutions. The general criteria for impalement validation were: (i) the potential differences (PDs) measured by both electrodes shanks should change abruptly, and the voltage deflections caused by the d.c. pulses should increase, (ii) after the stability of the PDs was reached, signals had to remain constant for at least 7 min (controls), (iii) finally the PDs should rapidly return to the respective baselines on leaving the cell. Voltage readings, after the beginning of impalement, were generally stable within 6–7 sec with the conventional channel and within 15–30 sec with the Cl^-- or Na^+-selective channel. During calibration signals from Cl^-- or Na^+-selective shanks were stable within about 12 sec. Na^+-sensitive microelectrodes were only used after bevelling.

Reverse Transcriptase (RT)-PCR

Rabbit gallbladder and ileum epithelial cells were obtained by scraping the mucosal surface with a glass slide; heart and liver were dissected in small pieces; immediately after that, all tissues were frozen in liquid nitrogen for subsequent homogenization. Total RNA was isolated by guanidine thiocyanate extraction followed by centrifugation in cesium chloride solutions [33]. $Poly(A)^+$ was purified from total RNA by affinity chromatography [33] using oligo(dT) cellulose (Amersham Pharmacia Biotech, Little Chalfont, UK). Reverse transcription was initiated by adding to each tube, containing 0.5 μg of $Poly(A)^+$ previously boiled for 1 min, a mix of 0.25 μg of hexamers (Boehringer, Mannheim, Germany), 120 U of M-MLV reverse transcriptase (Gibco BRL, Gaithersburg, MD), 10 nmol of dNTPs (Boehringer, Mannheim, Germany), 20 U of RNAse OUT inhibitor (Gibco BRL, Gaithersburg, Maryland) and 1 μl of 10X Taq buffer (Boehringer, Mannheim, Germany); the total volume was adjusted with sterile water to 10 μl. Samples were incubated for 10 min at room temperature and then for 1 hr at 37°C. The reaction was terminated by heating to 95°C for 5 min. Amplification was performed in the same tube, containing the previous 10 μl volume, by adding 40 μl of a mix containing 4 μl of 10X Taq buffer, 50 pmol of forward primer, 50 pmol of reverse primer, 1.25 U of Taq polymerase (Boehringer, Mannheim, Germany), 4 nmol of dNTPs and 33.3 μl of sterile water. The PCR reaction was performed in a RoboCycler Gradient 40 (Stratagene, La Jolla, CA) for 35 cycles, each one comprising 1 min denaturation step at 94°C, 1 min annealing phase at 50°C and 1 min of elongation at 72°C. The samples had previously undergone a prolonged denaturation step at 94°C for 5 min. A final prolonged elongation phase of 7 min at 72°C was also included in the protocol. We used nested TSC primer pairs (synthesised by Gibco Life Technologies, Glasgow, UK), designed on the base of the known rabbit kidney cDNA sequence (external pair: forward 5′-TACTGGCTCTTCGACGACGG-3′ reverse 5′-ATGACAGGGGGTCT GAGGTC-3′; region 2521–3038; product size 517 pb; internal pair: forward 5′-CACCCTCCTCATCCCCTACC-3′; reverse 5′-CTCCAGCCAGGCCATGTACA-3′; region 2547–3007, product size 461 bp). After a first RT-PCR performed using the external primers, the product obtained was used for a second PCR with the internal primer pair. Aliquots of the PCR products were run on 1.5% agarose gel in 1X TAE Buffer [33] and stained with a 0.2% ethidium bromide solution. The PCR fragments of interest were extracted from agarose gels (Gel Extraction Kit, Qiagen Gmbh, Hilden, Germany), ligated into $pCAP^s$ vector (PCR Cloning Kit blunt end, Boehringer, Mannheim, Germany) and sent to MWG-Biotech (Ebesberg, Germany) for double strand sequencing.

Salines

The Krebs-Henseleit saline used for the preliminary washings and the 30 min preincubation had the following composition (in mM: 142.9 Na^+, 5.9 K^+, 2.5 Ca^{2+}, 1.2 Mg^{2+}, 127.7 Cl^-, 24.9 HCO_3^-, 1.2 SO_4^{2-}, 1.2 $H_2PO_4^-$; pH 7.4. The bicarbonate-free saline (phosphate saline) contained (in mM): 145.3 Na^+, 6.0 K^+, 2.5 Ca^{2+}, 1.2 Mg^{2+}, 125.3 Cl^-, 13.7 SO_4^{2-}, 12.5 mannitol, 2.7 HPO_4^{2-}, 0.6 $H_2PO_4^-$; pH 7.4. Inhibitors were added directly to the solution (since the change in osmolality was negligible), with the exception of SCN^- (25 mM) which was substituted for 12.5 mM SO_4^{2-} and mannitol. HCTZ was directly dissolved in the saline and the final concentration was checked with a spectrophotometer (Lambda 5, Perkin Elmer, Norwalk, CT) at 226 nm. The salines were bubbled with 95% O_2 + 5% CO_2 (Krebs-Henseleit saline) or 100% O_2 (phosphate saline). The incubation temperature for all experiments was 27 ± 1°C.

SITS (4-acetamido-4′-isothiocyanostilbene-2,2′-disulfonate) and HCTZ were purchased from Sigma (St. Louis, MO), SCN^- from Carlo Erba Farmitalia (Milan, Italy). Alumina dry powder type B was purchased from Fisher, Fair Lawn, NJ.

STATISTICS

The results are reported as means ± SEM with the number of experiments in brackets. The one-way ANOVA test was used for statistical analysis; sometimes Student's *t*-test, generally with paired data analysis, was also used. The program "Enzfitter", version 1.05 (Elsevier Biosoft, Cambridge, UK) was used to calculate the parameters of the linear and nonlinear regressions. The BLAST protein data base search program [2] was used for sequence similarities.

Results

ANALYSIS OF Cl^- UPTAKE

As reported in the Introduction, with tissue bathed in bicarbonate/CO_2-free saline bubbled with 100% O_2, the apical Cl^- uptake is all HCTZ-sensitive and slowly abolished by the drug in 15 min; however, at this time a new bumetanide-sensitive uptake arises. In agreement with this finding, the apical Cl^- uptake per hr (μmol cm^{-2} hr^{-1}; measured in 45 sec, as in the past) was 10.7 ± 1.2 μmol cm^{-2} hr^{-1} (n = 18) under control conditions, decreased to 2.0 ± 0.8 and then increased again to 8.7 ± 0.7 μmol cm^{-2} hr^{-1} (n = 6 and 17, respectively) after 10 and 15 min treatments with 10^{-3} M HCTZ, the uptake at 15 min being completely bumetanide-sensitive. To establish whether the measured uptake per hour is the expression of an apical lumen to cell unidirectional influx (J_{mc}) or also includes an apical backflux, we investigated how long Cl^- entry into the cell (expressed as μmol cm^{-2}) increased linearly with measuring-time duration, after 15-min treatment with HCTZ. This treatment time was selected considering that after 15 min: (i) the HCTZ-induced apical G_{Cl} is maximally opened, (ii) the HCTZ-sensitive uptake is no longer detectable, (iii) yet the uptake is again high (because of the activation of the bumetanide-sensitive transport) thus allowing a significant analysis of the linearity of uptake *vs.* measuring-time length. The total, SCN^--sensitive (apical) and SCN^--insensitive (paracellular) Cl^- uptakes (μmol cm^{-2}) were measured, each one in 0, 30, 45 and 60 sec. Under control conditions (absence of treatment with HCTZ), a straight-line interpolated the data points up to 60 sec for total, apical and paracellular uptakes better than an exponential curve (Fig. 1 and Table). After 15 min treatment with 10^{-3} M HCTZ, the paracellular uptake increased linearly up to 60 sec as in the controls, which was to be expected since HCTZ does not modify paracellular selectivity [15]. However, the total and apical uptakes only increased linearly up to 45 sec (Fig. 2 and Table). Hence the measured apical uptakes per hour are related to unidirectional lumen-to-cell influxes (J_{mc}, expressed as μmol cm^{-2} hr^{-1}) up to 60 sec of measuring time under control conditions, but only up to 45 sec under treatment; however, the flux measured in 45 sec is unidirectional under both conditions and so always expresses only apical Cl^- entry into the cell without the influence of cell-to-lumen Cl^- backfluxes possibly caused by G_{Cl}.

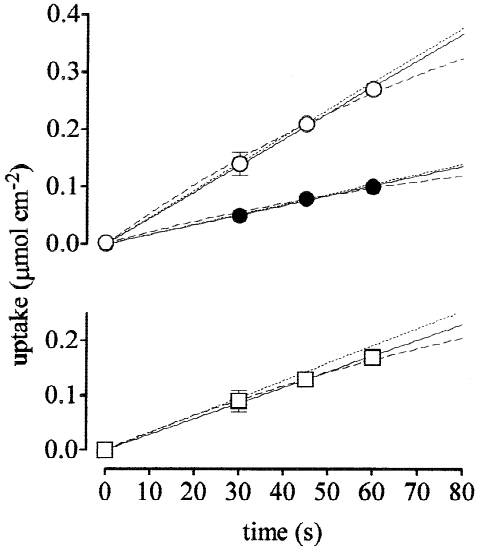

Fig. 1. Total, paracellular and cellular (apical) Cl^- uptake (μmol cm^{-2}) on the luminal side as a function of measuring time (s): control conditions. Analysis with linear and nonlinear regression to define the measuring time until which the uptake increases linearly and corresponds to the unidirectional lumen to cell influx (J_{mc}); n = 11 for each data point. Means ± SE. Uptake: total (○), paracellular (●), cellular (□). — straight-line calculated at 0, 30, 45, 60 sec; ···· straight line calculated at 0, 30, 45 sec; --- exponential curve calculated at 0, 30, 45, 60 sec.

As a countercheck that G_{Cl} did not interfere with the Cl^- uptake measurements performed in 45 sec, the epithelium was treated with 10^{-3} M HCTZ for 5 min. At this time: (i) G_{Cl} is largely, although not maximally, activated, (ii) the new bumetanide-sensitive influx is not yet homeostatically activated. The uptake decreased from the control value of 10.7 ± 1.2 μmol cm^{-2} hr^{-1} (n = 18) to 6.9 ± 1.0 μmol cm^{-2} hr^{-1} (n = 26). When G_{Cl} was prevented from activating by the concomitant treatment with 10^{-4} M SITS, the uptake was equally reduced to 6.4 ± 1.4 μmol cm^{-2} hr^{-1} (n = 11). Thus the presence or absence of G_{Cl} did not interfere with uptake inhibition by HCTZ.

INTRACELLULAR Cl^- AND Na^+ ACTIVITIES

The apical membrane potential (V_m) and the intracellular Cl^- or Na^+ activities ($a_{i,Cl}$, $a_{i,Na}$) were measured concomitantly in the same cell by theta-microelectrodes. The intracellular recordings were similar to those already reported for both Cl^- and Na^+ measurements [16, 27]. Figures 3*A* and 4*A* show two examples. One of the two tracings measured simultaneously refers to V_m and the second directly to the apparent chemical potential differ-

Table. Linear and nonlinear regressions of total, paracellular and cellular (apical) Cl^- uptake on the luminal side against measuring time, under control conditions (A) or treatment with 10^{-3} M HCTZ for 15 min (B)*

Uptake	Straight-line (on 0, 30, 45 sec)	Straight-line (on 0, 30, 45, 60 sec)	Exponential curve (on 0, 30, 45, 60 sec)
A			
Total	$y = 47.2 \times 10^{-4}x$	$y = 45.9 \times 10^{-4}x$	$y = 6358.4 \times 10^{-4}[1\text{-}e^{-89.4\times10^{-4}x}]$
r^2	1	0.995	0.879
Paracellular	$y = 17.4 \times 10^{-4}x$	$y = 17.0 \times 10^{-4}x$	$y = 2102.7 \times 10^{-4}[1\text{-}e^{-102.9\times10^{-4}x}]$
r^2	0.983	0.986	0.916
Cellular	$y = 31.9 \times 10^{-4}x$	$y = 28.8 \times 10^{-4}x$	$y = 4506.6 \times 10^{-4}[1\text{-}e^{-76.1\times10^{-4}x}]$
r^2	0.990	0.994	0.889
B			
Total	$y = 43.7 \times 10^{-4}x$	$y = 42.2 \times 10^{-4}x$	$y = 5312.0 \times 10^{-4}[1\text{-}e^{-101.0\times10^{-4}x}]$
r^2	0.934	0.858	0.864
Paracellular	$y = 17.4 \times 10^{-4}x$	$y = 18.3 \times 10^{-4}x$	$y = 4022.7 \times 10^{-4}[1\text{-}e^{-51.5\times10^{-4}x}]$
r^2	0.946	0.975	0.899
Cellular	$y = 25.3 \times 10^{-4}x$	$y = 23.9 \times 10^{-4}x$	$y = 2705.7 \times 10^{-4}[1\text{-}e^{-115.4\times10^{-4}x}]$
r^2	0.932	0.823	0.870

* Uptake (y: μmol cm^{-2}) is shown as a function of measuring time length (x: sec). The measuring time was 0, 30, 45, 60 sec. Experimental points and interpolations are reported in Figs. 1 and 2; the corresponding equations and r^2 are reported in the Table. Under control conditions a straight line interpolates the data points up to a measuring time of 60 sec better than an exponential curve for total, paracellular and cellular uptake (higher r^2). Under treatment, the cellular uptake data points are better interpolated by a straight line only up to 45 sec.

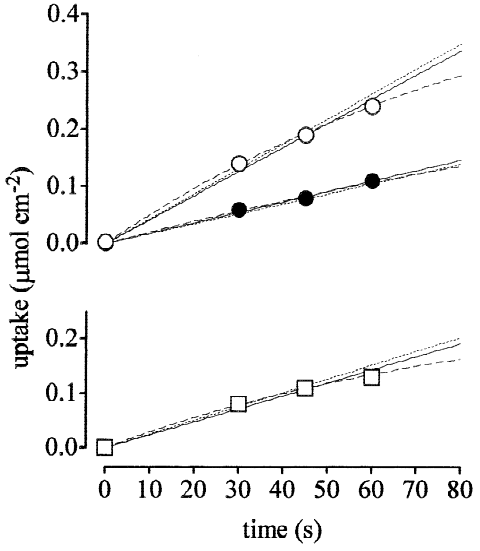

Fig. 2. Total, paracellular and cellular (apical) Cl^- uptake (μmol cm^{-2}) on the luminal side as a function of measuring time (s): HCTZ treatment. Analysis with linear and nonlinear regression to define the measuring time until which the uptake increases linearly and corresponds to the unidirectional lumen to cell influx (J_{mc}), after 10^{-3} M HCTZ treatment for 15 min; $n = 14$ for each data point. Means ± SE. Uptake: total (○), paracellular (●), cellular (□). — straight line calculated at 0, 30, 45, 60 sec; ···· straight line calculated at 0, 30, 45 sec; --- exponential curve calculated at 0, 30, 45, 60 sec.

ence (Δμ) for Cl^- or Na^+, respectively, as the electrometer was set to automatically subtract the membrane potential, measured by the conventional channel, from the electrochemical potential difference measured with the ion-selective channel. On the overall number of 7 min impalements performed, during the first min (control) V_m was −67.0 ± 0.3 mV ($n = 174$), $a_{i,Cl}$ 25.4 ± 0.6 mM ($n = 94$), $a_{i,Na}$ 16.7 ± 0.8 mM ($n = 80$) in accordance with previous data [12, 13, 16]; $a_{i,Cl}$ was 3.6 times greater than predicted at the electrochemical equilibrium. The variations in $a_{i,Cl}$ and $a_{i,Na}$ during the treatment and post-treatment periods (3 + 3 min) were calculated by reference to the activity measured during the first min of impalement, taken as zero.

In a first set of experiments ($n = 35$) the stability of $a_{i,Cl}$ and $a_{i,Na}$ was tested during 7 min single impalements under control conditions. As shown in Fig. 5, the mean variations in $a_{i,Cl}$ and $a_{i,Na}$ were nil. Figures 3*A* and *B*, and 4*A* and *B* report examples of the $\Delta\mu_{Cl}$ and $\Delta\mu_{Na}$ tracings, which were stable under control conditions. The apical membrane potential was equally stable (Figs. 3*A* and 4*A*).

In a second set of experiments ($n = 16$), we investigated whether under the conditions used (HCO_3^-/CO_2-free salines, bubbled with 100% O_2) no residual Cl^-/HCO_3^- exchange was detectable, as predicted from previous observations [12, 14]. As shown in Fig. 5, 10^{-4} M SITS did not reduce $a_{i,Cl}$. An example of the $\Delta\mu_{Cl}$ tracing under these conditions is shown in Fig. 3*D*. V_m was equally unaffected (*unpublished results*).

In a third set of experiments ($n = 17$) the effects of luminal 10^{-4} M HCTZ were tested. V_m variations due to HCTZ were represented by small decreases (less than 1 mV), which were significant but transient, as already described [18], so they are not reported. Both $a_{i,Cl}$ and $a_{i,Na}$ decreased during treatment in 3 min by 1.6 ± 1.0 and 0.8 ± 0.4 mM, respectively, but the decrease was not statistically significant. Some further impalements with

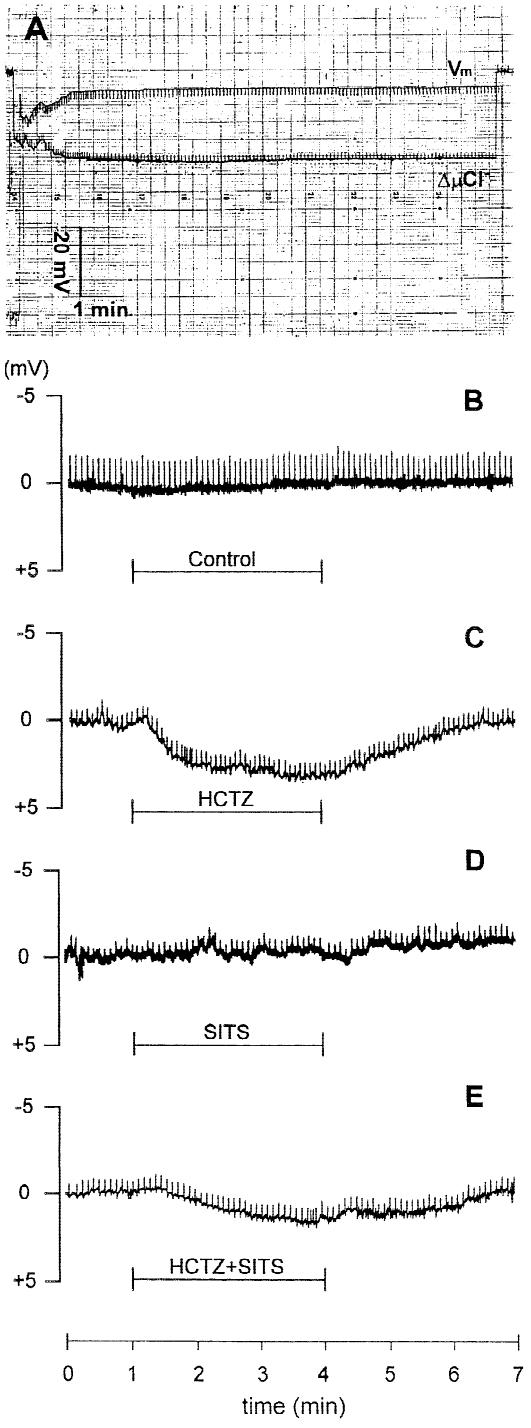

Fig. 3. Examples of tracings recorded in the same cell with theta microelectrodes, with a Cl^--selective channel and a conventional channel to measure V_m. Since the electrometer was set to automatically subtract the membrane potential V_m, measured by the conventional channel, from the electrochemical potential difference, measured by the ion-selective channel, the voltage change tracing, recorded by the latter, represents the apparent chemical potential difference for Cl^- ($\Delta\mu_{Cl}$). (A) complete recordings of V_m and $\Delta\mu_{Cl}$ during an impalement lasting 7 min after stability was obtained. (*B*) $\Delta\mu_{Cl}$ tracing under control conditions. (*C*) $\Delta\mu_{Cl}$ tracing under control conditions (1 min), 10^{-4} M SITS (3 min), control conditions again (last 3 min). (*D*) $\Delta\mu_{Cl}$ tracing under control conditions (1 min), 2.5×10^{-4} M HCTZ (3 min), control conditions again (last 3 min). (*E*) $\Delta\mu_{Cl}$ tracing under control conditions (1 min), 2.5×10^{-4} M HCTZ $+10^{-4}$ M SITS (3 min), control conditions again (last 3 min). The bars indicate the period of solution renewal (control) or the treatment period.

Cl^--selective theta microelectrodes ($n = 4$) were prolonged for more than 15 min; treatment started after 1 min and lasted for 15 min. The Cl^- activity progressively decreased by 4.0 ± 2.0 mM in 15 min, but the decrease was only marginally significant. Thus with 10^{-4} M HCTZ, V_m undergoes an initial significant decrease which, however, is transient, whereas $a_{i,Cl}$ and $a_{i,Na}$ undergo only slow, marginally significant decreases.

More clear-cut results were obtained by treating the tissue with 2.5×10^{-4} M HCTZ on the luminal side ($n = 24$).

V_m started to decrease within 10 sec after the beginning of the treatment; the extent of the decrease and the time course were in agreement with those previously measured at the same HCTZ concentration [18], so they are not reported again. Figures 3*C* and 4*C* show examples of the $\Delta\mu_{Cl}$ and $\Delta\mu_{Na}$ tracings recorded before, during and after treatment with 2.5×10^{-4} M HCTZ. As shown in Fig. 6, both $a_{i,Cl}$ and $a_{i,Na}$ started to decrease within 20 sec after beginning of the treatment; this delay may have been related to the saline renewal in the chamber (4–5 sec), the unstirred apical layers, the response time of the selective microelectrode and the time lag between membrane and intracellular changes. After 3 min of treatment, $a_{i,Cl}$ was reduced significantly by 4 mM and $a_{i,Na}$ by about 2 mM; the effect was reversible and, 3 min after the end of the treatment, the values were again at control level. During treatment the $a_{i,Cl}$ decrease was larger than that of $a_{i,Na}$ at $P < 0.05$ level until 1 min, and at $P < 0.01$ level at 2 and 3 min. In the used range of the calibration curve, 1 mV corresponded to about 1 mM for Cl^- and 0.5 mM for Na^+; hence the observed decrease of 4 mM for Cl^- and 2 mM for Na^+ corresponded to a reduction of 4 mV in both cases and the error was similar. Moreover, since after bevelling the response time was not significantly different for Cl^-- and Na^+-selective microelectrodes, this possible explanation of the discrepancies between the decrease in intracellular Cl^- and Na^+ activities was also ruled out.

Knowing that G_{Cl}, activated by 2.5×10^{-4} M HCTZ, is abolished by SITS, the treatment was repeated with HCTZ and 10^{-4} SITS present together ($n = 15$). Figure 3*E* and 4*D* show examples of the corresponding effects on the $\Delta\mu_{Cl}$ and $\Delta\mu_{Na}$ tracings. Figure 6 reports that under these conditions the decrease in $a_{i,Na}$, elicited by

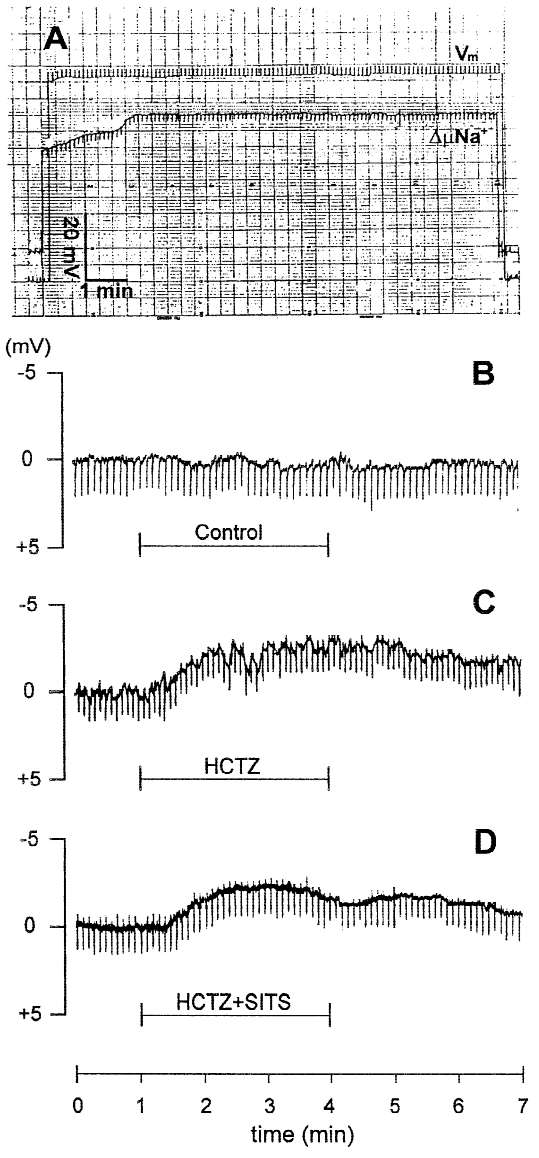

Fig. 4. Examples of tracings recorded in the same cell with theta microelectrodes, with a channel selective to Na^+ and a conventional channel to measure V_m. Since the electrometer was set to automatically subtract the membrane potential V_m, measured by the conventional channel, from the electrochemical potential difference, measured by the ion-selective channel, the voltage change tracing, recorded by the latter, represents the apparent chemical potential difference for Na^+ ($\Delta\mu_{Na}$). (*A*) complete recordings of V_m and $\Delta\mu_{Na}$ during an impalement lasting 7 min after stability was obtained. (*B*) $\Delta\mu_{Na}$ tracing under control conditions. (*C*) $\Delta\mu_{Na}$ tracing under control conditions (1 min), 2.5×10^{-4} M HCTZ (3 min), control conditions again (last 3 min. (*D*) $\Delta\mu_{Na}$ tracing under control conditions (1 min), 2.5×10^{-4} M HCTZ $+10^{-4}$ M SITS (3 min), control conditions again (last 3 min). The bars indicate the period of solution renewal (control) or the treatment period.

HCTZ, was not significantly affected by SITS at any time. By contrast, $a_{i,Cl}$ activity decreased significantly less at every time than with HCTZ alone (P at least < 0.05 at each data point); the maximal effect was a decrease of about 2 mM in 3 min. Under these conditions the $a_{i,Cl}$ decrease was not significantly different from that of $a_{i,Na}$ at any time. Hence, although G_{Cl} was abolished, $a_{i,Cl}$ and $a_{i,Na}$ still decreased, but now with a 1:1 rate, as predicted for the inhibition of electroneutral symport. Activity decreases are better quantified as initial rates of decrease per min (IRDs), measured on the basis of the linear activity drop observed between 20 and 30 sec after

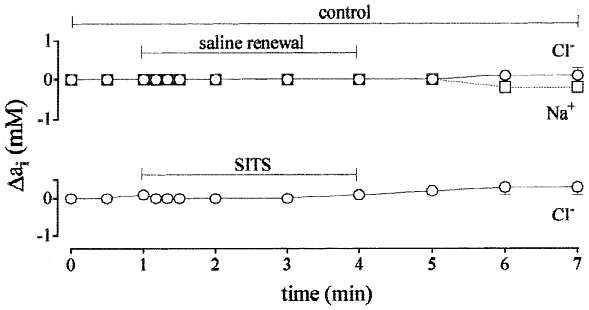

Fig. 5. Intracellular Cl^- and Na^+ activities under control conditions or treatment with 10^{-4} M SITS. Values are reported as means ± SE of the variations in Cl^- and Na^+ activities ($\Delta a_{i,Cl}$, $\Delta a_{i,Na}$) measured during single 7 min impalements; the control values during the first min, before saline renewal (control) or treatment with SITS, are taken as reference zero; they also are reference for the control values in the final 3 min. Number of impalements: 15 (control), 16 (SITS). No $\Delta a_{i,Cl}$ or $\Delta a_{i,Na}$ was significant. —○—: $\Delta a_{i,Cl}$; ⋯ ⋯: $\Delta a_{i,Na}$.

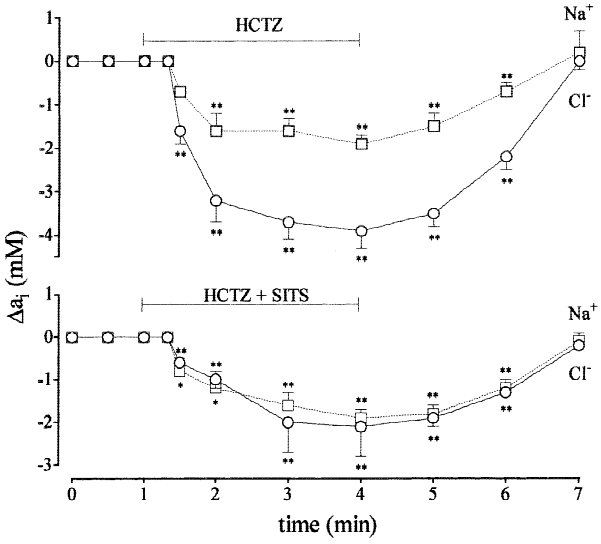

Fig. 6. Decrease in intracellular Cl^- and Na^+ activities ($\Delta a_{i,Cl}$, $\Delta a_{i,Na}$) after luminal treatment with HCTZ or HCTZ and SITS concomitantly. The variations, reported as means ± SE were measured during single impalements prolonged for 7 min. The control values (1st min) before treatment are taken as reference zero; they also are reference for the control values in the final 3 min. Number of impalements under the two treatment conditions: 13 and 9 for $\Delta a_{i,Cl}$, 11 and 6 for $\Delta a_{i,Na}$. *, **: P < 0.05 for 0.01 compared with control before treatment. —○—: $\Delta a_{i,Cl}$, ⋯ ⋯: $\Delta a_{i,Na}$.

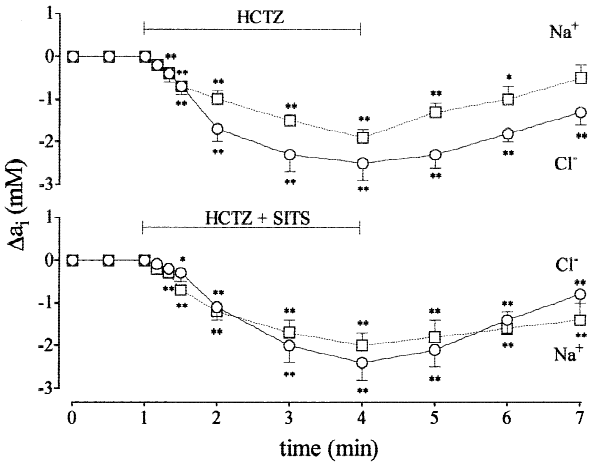

Fig. 7. Gallbladders with low HCTZ-elicited G_{Cl}: decrease in intracellular Cl^- and Na^+ activities ($\Delta a_{i,Cl}$, $\Delta a_{i,Na}$) after luminal treatment with HCTZ or HCTZ and SITS concomitantly. The variations, reported as means ± SE, were measured during single impalements prolonged for 7 min. The control values (1st min) before treatment are taken as reference zero; they also are reference for the control values in the final 3 min. Number of impalements under the two treatment conditions: 16 and 17 for $\Delta a_{i,Cl}$, 20 in both cases for $\Delta a_{i,Na}$. *, **: $P < 0.05$ or 0.01 compared with control before treatment. —○—: $\Delta a_{i,Cl}$; ⋯ ⋯: $\Delta a_{i,Na}$.

the beginning of the treatment, so as to detect intracellular changes only due to modifications at the apical membrane. Under HCTZ treatment, the IRD for Cl^- was larger than for Na^+ (9.6 ± 1.8 and 4.4 ± 0.4 mM/min, n = 13 and 11, respectively; $P < 0.05$). Under HCTZ and SITS treatment IRD_{Cl} decreased significantly ($P < 0.05$) to 3.3 ± 0.8 mM/min (n = 9), and became not significantly different from IRD_{Na} which, conversely, did not change (4.8 ± 1.8 mM/min, n = 6). These results confirm that a component of the HCTZ-induced $a_{i,Cl}$ decrease is SITS-sensitive, whereas the second component is SITS-insensitive and equal to the HCTZ-induced $a_{i,Na}$ decrease.

In another group of gallbladders the total depolarization caused by 2.5×10^{-4} M HCTZ within 3 min was much less than normal, and the G_{Cl} about one-third (for this evaluation *see* ref. 18). This fact offered the opportunity of observing the effect of a naturally reduced G_{Cl} on the $a_{i,Cl}$ and $a_{i,Na}$ decreases. Figure 7 shows the $\Delta a_{i,Cl}$ and $\Delta a_{i,Na}$ elicited by HCTZ under these conditions: $a_{i,Cl}$ decreased by 2.5 mM and $a_{i,Na}$ by 1.9 mM within 3 min ($P < 0.01$ for both variations, n = 16 and 20, respectively). The discrepancy between the $a_{i,Cl}$ and $a_{i,Na}$ variations was only significant after 1 min of treatment ($P < 0.05$). It was reduced to about 0.6 mM (namely to less than one third) compared with 2.0 mM in the previous group of gallbladders with normal G_{Cl} ($P < 0.05$). As in the previous group, the discrepancy between the $a_{i,Cl}$ and $a_{i,Na}$ decreases was abolished by treating concomitantly with 10^{-4} M SITS to eliminate G_{Cl} (Fig. 7). $\Delta a_{i,Na}$ was unaffected at each data point ($\Delta a_{i,Na}$ = 2.0 mM after 3 min of treatment, n = 20); it was the $a_{i,Cl}$ variation which decreased to overlap with that of $a_{i,Na}$ (n = 17).

In conclusion, the rate of $a_{i,Na}$ decrease was independent of the extent of G_{Cl} and only dependent on HCTZ concentration. Conversely, the rate of $a_{i,Cl}$ decrease displayed two components; the first was not significantly different from the rate of $a_{i,Na}$ decrease and was independent of G_{Cl}; the second was related to the presence and extent of G_{Cl}.

RT-PCR Analysis

To ascertain whether the NaCl cotransporter demonstrated in rabbit gallbladder is similar to the kidney thiazide sensitive isoform (TSC), we performed an RT-PCR analysis on the mRNA of gallbladder epithelium. The same analysis was performed on mRNA of kidney cortex, ileum, heart and liver to get information on the relative level of expression of the cotransporter. Nested primers were designed on the basis of the known cDNA sequence of rabbit kidney TSC, in order to amplify a fragment which was expected to be in the presumed cytoplasmic C terminal region, one of the most conserved and representative of the subfamily, distinguishing it from the other members of the Cation Chloride Cotransporter family. To obtain information on tissue distribution and level of expression of TSC mRNA, RT-PCR experiments were performed by using external primers and same amounts of $poly(A)^+$ obtained from kidney cortex (used as positive control), gallbladder epithelium, ileum epithelium, heart and liver (used as negative controls). To rule out possible contaminations in the RT-PCR experiments, controls with water instead of $poly(A)^+$ in the RT reaction were performed in parallel. Moreover, in order to exclude contamination by genomic DNA, as no genomic sequence is available for rabbit TSC, although the analysis of the reported sequence for the human TSC gene [35] indicates that the chosen primer pair might possibly span more than one intron, an additional negative control with RNA was also set up, but without reverse transcriptase in the RT reactions. In all the RT-PCR experiments (n = 4) no bands were detectable in either of the negative controls. RT-PCR products from all tissues (10 μl each) were run on gel electrophoresis; staining with ethidium bromide allowed detection of two bands for kidney, gallbladder and intestine tissues, one of them of the expected size (517 bp, Fig. 8, Panel *A*). No band of the same size was detected for heart and liver (Fig. 8, Panel *B*). Densitometric analysis of the bands of the expected size, assuming kidney cortex as 100% reference, was 58 and 36% for gallbladder and intestine, respectively. Products obtained with the external primer pair were reamplified by PCR

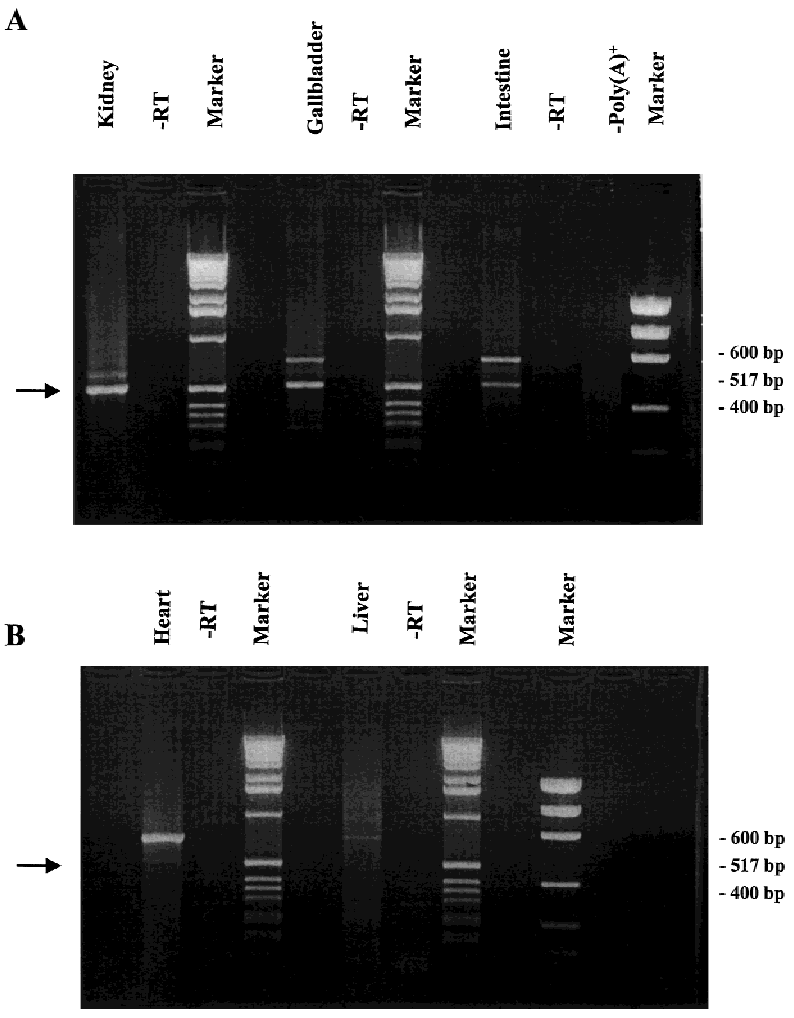

Fig. 8. PCR amplification of TSC mRNA in various rabbit tissues. RT-PCR was performed injecting 0.5 μg of poly(A)$^+$ isolated from different rabbit tissues. The amplified PCR products (external primers) were detected on 1.5% agarose gel, stained with ethidium bromide. In panel *A* a band of the expected size (517 bp, indicated by the arrow) was detected in lanes 1 (kidney cortex), 5 (gallbladder epithelium) and 9 (ileum epithelium). Lanes 2, 6 and 10 show the negative controls: same RT-PCR mix without reverse transcriptase. Lane 11 shows some RT-PCR mix without poly(A)$^+$. The double strand DNA molecular weight marker is in lane 3 and 7; mass ladder marker is in lane 12. In panel *B* no band of the expected size (indicated by the arrow) was detected. Lanes 2 and 6 show products obtained starting from heart and liver poly(A)$^+$. Lanes 3 and 7 show negative controls without reverse transcriptase. Molecular weight marker (1 Kb DNA ladder, Gibco BRL, Gaithersburg, MD) is in lane 4 and 8. Mass ladder marker (Low DNA Mass™, Ladder, Gibco BRL, Gaithersburg, MD) is in lane 10.

using the internal primers. Gel electrophoresis of products from kidney, intestine and gallbladder evidenced one product which resulted of the expected size. No products were observed when internal nesting was done on RT-PCR products from heart and liver. To assess product specificity, the gallbladder cDNA was subcloned in the pCAP^s vector (*see* Materials and Methods section) and sequenced. The sequence showed a very high homology with the corresponding region of the kidney isoform (99%).

Alignment (Fig. 9) of the derived amino acid sequence with the corresponding region of cloned NaCl cotransporters shows an identity ranging from 91% (rat kidney) to 99% (rabbit kidney) with the other mammalian isoforms. Considering positivities between amino acids as well as identities, the percentage is 98% on average. As for the rabbit kidney isoform, the only difference is the amino acid sequence compared with the corresponding segment of rabbit gallbladder TSC is in position 995 (position 155 of the rabbit gallbladder fragment), which presents a serine instead of a threonine due to a change in the first base of the codon (TCC instead of ACC).

Discussion

All the results reported here are in agreement in showing that HCTZ directly inhibits apical Na^+-Cl^- symport, although it concomitantly opens the apical Cl^- leak.

Analysis of Cl^- Uptake

Apical Cl^- uptake, measured with $^{36}Cl^-$ and expressed as μmol cm^{-2}, is predicted to increase exponentially with length of measuring time to a final steady-state value, which is reached when the influx is equal to the apical and basolateral effluxes. With short measuring time lengths (owing to cell volume: some tens of seconds) the apical Cl^- uptake must increase linearly as long as $^{36}Cl^-$ losses through the apical and basolateral membranes re-

```
Rabbit gallbladder      1 YWLFDDGGLTLLIPYLLGRKKRWSRCKIRVFVGGQINRMDQERKAMVSLLSKFRLGFHEV
Rabbit kidney         841 YWLFDDGGLTLLIPYLLGRKKRWSRCKIRVFVGGQINRMDQERKAMVSLLSKFRLGFHEV
Man kidney            834 YWLFDDGGLTLLIPYLLGRKRRWSKCKIRVFVGGQINRMDQERKAIISLLSKFRLGFHEV
Rat kidney            815 YWLFDDGGLTLLIPYLLHRKKRWGKCKIRVFVGGQINRMDEERKAIISLLSKFRLGFHEV
Mouse kidney          814 YWLFDDGGLTLLIPYLLHRKKRWGKCKIRVFVGGQINRMDEERKAIISLLSKFRLGFHEV
Winter f. bladder     834 YWLSDDGGLTLLLPYLLTRRKRWAGCKVRVFVGGDTDKKEEQKEEVLALIKKFRLGFHDV

Consensus               1 YWLfDDGGLTLLiPYLLgRkkRWskCKiRVFVGGqinrmd erkaiisLlsKFRLGFHeV


Rabbit gallbladder     61 HVLPDINQKPRAEHTKRFEDMIAPFRLNDGFKDEATVAEMRR--DCPWKISDEEINKNRI
Rabbit kidney         901 HVLPDINQKPRAEHTKRFEDMIAPFRLNDGFKDEATVAEMRR--DCPWKISDEEINKNRI
Man kidney            894 HILPDINQNPRAEHTKRFEDMIAPFRLNDGFKDEATVNEMRR--DCPWKISDEEITKNRV
Rat kidney            875 HVLPDINQKPQVEHTKRFEDMIAPFRLNDGFKDEATVAEMRR--DYPWKISDEEINKNRI
Mouse kidney          874 HVLPDINQKPQAEHTKRFEDMIAPFRLNDGFKDEATVTEMRR--DCPWKISDEEINKNRI
Winter f. bladder     894 EVLPDIHQPPQPGNVDHFEDSVNRFRLETNPKQDSDSGPQQQQQEEPWMITEQDLERNRA

Consensus              61 hvLPDInQkP aehtkrFEDmiapFRLndgfKdeatvaemrr  dcPWkIsdeeinkNRi


Rabbit gallbladder    119 KSLRQVRLNEILLDYSRDAALVVITLPIGRKGKCPSSLYMAWLETLSQDLRPPVI
Rabbit kidney         959 KSLRQVRLNEILLDYSRDAALVVITLPIGRKGKCPSSLYMAWLETLSQDLRPPVI
Man kidney            952 KSLRQVRLNEIVLDYSRDAALIVITLPIGRKGKCPSSLYMAWLETLSQDLRPPVI
Rat kidney            933 KSLRQVRLNEILLDYSRDAALIILTLPIGRKGKCPSSLYMAWLETLSQDLSPPVL
Mouse kidney          932 KSLRQVRLSEILLDYSRDAALIILTLPIGRKGKCPSSLYMAWLETLSQDIRPPVL
Winter f. bladder     952 KSLRQIRLNEVLQVHSREAALIVITMPVGRRGVCPSTLFLAWLDVLSRDLRPPVL

Consensus             121 KSLRQvRLnEilldySRdAALiviTlPiGRkGkCPSsLymAWLetLSqDlrPPVi
```

Fig. 9. Alignment of the deduced partial amino acid sequences of the Na^+-Cl^- cotransporter TSC. The animal organ, Data Bank with accession number and identity percentage with the deduced partial sequence of rabbit gallbladder are as follows: Rabbit kidney, GenBank AF028241, 99%; Man kidney, GenBank U44128, 93%; Rat kidney, GenBank U10097, 91%; Mouse kidney, GenBank U61085, 91%; Flounder urinary bladder, GenBank L11615, 53%. The shadowed amino acids indicate differences between rabbit kidney and gallbladder sequences.

main negligible. Until this time, the measured uptake per hour (μmol cm^{-2} hr^{-1}) expresses the unidirectional influx J_{mc}, whereas after this time it expresses a net flux. Under control conditions no G_{Cl} is apically present (*see* Introduction), so that $^{36}Cl^-$ losses only start to be significant when the $^{36}Cl^-$ accumulated intracellularly is sufficient to cause a significant basolateral $^{36}Cl^-$ exit, as well as the very limited apical backflux through the Na^+-Cl^- symporter [15]. The results reported show that under these conditions $^{36}Cl^-$ loss is not significant, at least up to a 60-sec measuring time, in agreement with previous observations [9]. Under treatment with HCTZ, the G_{Cl} opening increases the apical Cl^- leaks, and with a 60-sec measuring time the $^{36}Cl^-$ loss becomes significant. In any event, with a 45-sec measuring time the determined uptake corresponds to the unidirectional influx J_{mc} under both control and treatment conditions. Thus its inhibition by HCTZ is inhibition of the Cl^- entry into the cell only, without interference by a conductive backflux. Moreover, under treatment conditions, even with a 60-sec measuring time, the deviation from linearity of the uptake against measuring time length, though present, is minimal, and could only account for the disappearance of an uptake of 1.4 and not 10 μmol cm^{-2} hr^{-1}, as required to account for the disappearance of the total HCTZ-sensitive uptake. As a countercheck, the concomitant G_{Cl} abolition with SITS does not affect the extent of the uptake inhibition by HCTZ. The necessary conclusion of all these observations is that HCTZ directly inhibited the symport, as well as opening the parallel G_{Cl}.

Intracellular Cl^- and Na^+ Activities

In the absence of Na^+/H^+,Cl^-/HCO_3^- double exchange, the apical NaCl entry is roughly halved. Under these conditions about 97% of the apical Na^+ entry is neutrally coupled to Cl^- on the Na^+-Cl^- symporter; the remaining 3% occurs through a conductive Na^+ pathway [13]. All the Cl^- entry takes place by the symport with Na^+ [7, 11, 12, 14, 23]. After HCTZ treatment, the opening of the SITS-sensitive apical Cl^- conductance should favor the apical exit of Cl^- accumulated intracellularly by the symport above the value predicted for the Cl^- electrochemical equilibrium. If this were the only action exerted by HCTZ and the symport were hypothetically unaffected, intracellular Cl^- activity should decrease at a rate completely blockable by SITS; meanwhile, Na^+ should continue to enter the cell by the unaffected symport, so its intracellular activity should not decrease. The reduction

of intracellular Cl^- activity should inhibit basolateral Cl^- exit, which occurs through a neutral pathway [7, 13, 23] identified in *Necturus* gallbladder with a KCl symport [5, 31, 32]. This would indirectly reduce Na^+ pumping, with consequent: (i) inhibition of transepithelial NaCl transport, (ii) increases in cytoplasmic Na^+ activity. Clearly this is not what happens. In fact, only part of the rate of $a_{i,Cl}$ decrease is SITS-blockable, and intracellular Na^+ activity decreases in parallel with Cl^- at a rate equal to that of the SITS-insensitive Cl^- fraction. These observations are in line with a dual action of HCTZ, consisting of both $a_{i,Cl}$ activation and Na^+-Cl^- symport inhibition.

This conclusion is strengthened by the results obtained on the set of gallbladders in which HCTZ only elicited a low G_{Cl}, equal to about one-third of that observed in the first set (and normally observed previously). In this case the SITS-sensitive fraction of the rate of $a_{i,Cl}$ decrease was reduced to about one-third of the corresponding fraction of the first set. Conversely, the SITS-insensitive fraction remained equal in both groups and maintained a 1:1 ratio with the rate of $a_{i,Na}$ decrease, as predicted for direct inhibition of the symport.

Equally, the corresponding initial rates of $a_{i,Na}$ and SITS-insensitive $a_{i,Cl}$ decreases were not significantly different, thus indicating simultaneous inhibition of Na^+ and Cl^- influxes, again in agreement with symport inhibition. These rates proved much lower than those previously measured under conditions of instantaneous complete block of symport [12]. This is in agreement with the slow development of symport inhibition by HCTZ [16].

An apparent contradiction deserves some comments. Radiochemical measurements showed that, when G_{Cl} is maximally opened, Cl^- backflux is negligible for at least 45 sec; on the other hand intracellular Cl^- activity measurements showed that, when G_{Cl} is only starting to open, a significant Cl^- backflux occurs in 10 sec, as a significant SITS-sensitive decrease of intracellular Cl^- activity is already detected after this time. The contradiction is only apparent since in the former case the backflux concerns $^{36}Cl^-$ and the Cl^- labeled by it (for at least 45 sec the $^{36}Cl^-$ accumulated in the cell is negligible in order to generate a substantial backflux); in the latter case the backflux concerns Cl^- (in the cell, Cl^- activity is about 25 mM, so that on activation of G_{Cl} the backflux depending on it can immediately be generated).

Finally, it should be emphasized that on treatment the rates of $a_{i,Cl}$ and $a_{i,Na}$ decreases were initially high, but after 10 sec always slower, in line with the fact that, at the beginning, intracellular ion reductions are only related to modifications at the apical membrane (*see* IRD), but subsequently the substantial decreases reached in intracellular activities reduce the rates of basolateral exits; $a_{i,Cl}$ was shown to decrease towards the electrochemical equilibrium value, though at a slower rate owing to this cause, with a minimum reached 15–30 min after treatment [16].

Molecular Identification of the Na^+-Cl^- Cotransporter

Thiazide sensitive Na^+-Cl^- cotransporters belong to a subfamily which is part of the major family of the Cation-Chloride Cotransporters (CCC), which includes the Na^+-K^+-$2Cl^-$ and K^+-Cl^- cotransporters [28]. Selective inhibition with thiazides has been a primary tool for their functional identification for many years. Since the first cloning of a TSC member from winter flounder urinary bladder [22], other isoforms have been cloned, all located at the distal convoluted tubule of mammalian kidney. They are in the apical membrane of the cell, where they represent the main Na^+ and Cl^- entry pathway and are the target of thiazide diuretics [35]. Though usually referred to as "kidney specific" [25, 29], there are indications of the presence of low levels of TSC transcripts in non renal tissues, though the relationship between expression and physiological role has not been elucidated in any of these tissues [4, 21, 22], with the exceptions of a human osteoblast like cell line [3] and human peripheral blood mononuclear cells [1]. As for the isoform we identified in rabbit gallbladder, we performed a semi quantitative analysis of the corresponding mRNA presence in different tissues. Kidney cortex showed the highest expression while the presence of the TSC mRNA in liver and heart could not be detected as already found in man and rat [4, 21, 25]. The 58% expression found for gallbladder epithelium relative to kidney is consistent with a functional expression of TSC in this tissue; also the amount of mRNA found in the ileum (36% relative to the kidney) is a suggestion that the cotransporter might play a functional role in this tract of intestine. The question deserves investigation since indications of TSC presence in intestine, but not of its role, has already been reported for man and rat [4, 21, 22]. Thus perhaps, the original suggestions concerning the presence of a ternary complex (Na^+, Cl^-, carrier) in rabbit ileum, presented by Nellans, Frizzell and Schultz (1973) [30], should be reconsidered.

In rabbit gallbladder, the high similarity of the cDNA sequence of the fragment obtained by PCR with the corresponding sequences of the cloned TSC transporters is a clear indication that it belongs to the same subfamily. In particular, it is practically identical to the corresponding region of the rabbit kidney isoform, with only 3 different bases (fragment length: 519 bp). The only base change resulting in an amino acid difference is at position 465 of our sequence (A in the gallbladder sequence, T in the kidney sequence). Anyway the different residues (threonine in gallbladder sequence sub-

stituting for serine, due to the mutation of the first base in the corresponding condon) are positively correlated (BLAST analysis). Moreover, a serine residue is also present in the corresponding position of the flounder sequence and is codified by the same codon present in rabbit gallbladder cDNA fragment. Yet considering the fact that splicing isoforms with still unknown functional implications are reported for other animals [21, 24], complete identity with the kidney isoform could only be established by analyzing the whole cDNA, including the 3′ untranslated region.

Conclusions

To sum up, although HCTZ activates an apical G_{Cl}, through which a cell-to-lumen apical Cl^- backflux occurs, thus contributing to a reduction in $a_{i,Cl}$, HCTZ also directly inhibits the Na^+-Cl^- symporter present in rabbit gallbladder epithelium; moreover, molecular data confirm the presence of a TSC. This is the first evidence of the functional expression of a TSC in a nonrenal or nonrenal-like epithelium. Rabbit gallbladder epithelium was one of the first two tissues in which passive (or secondary active) electroneutral NaCl transport was demonstrated; moreover, it was the first one for which the ternary complex model (symport model) was proposed to account for the functioning of electroneutral transport [7, 8, 20, 23], later confirmed by experimental evidence [11, 12, 14]. It is now clear that this symport belongs to the TSC subfamily, which has meanwhile been studied extensively in renal and renal-like epithelia.

Conversely, with the present data, it cannot be ascertained whether the isoform shown here is identical or only similar to the renal isoform. Some physiological observations seem to indicate a number of differences. The HCTZ concentration necessary to obtain complete inhibition is apparently 6–7 times higher [16]; however, many uncertainties in the determination of the dose-response curve (rapid homeostatic activation of a bumetanide sensitive Na^+-K^+-$2Cl^-$ cotransport; dependence of the HCTZ action on the bivalent anions present in the incubation saline) make this point still unclear [16, 17]. The time required to complete the inhibition also seems to be longer in gallbladder (10–15 min *vs.* 3 min at most [26, 36]); however, under certain conditions it seems that it can be considerably shortened [17, 26]. Thus further information is required to clarify this point.

References

1. Abuladze, N., Yanagawa, N., Lee, I., Jo, O.D., Newman, D., Hwang, J., Uyemura, K., Pushkin, A., Modlin, R.L., Kurtz, I. 1998. Peripheral blood mononuclear cells express mutated NCCT mRNA in Gitelman's syndrome: evidence for abnormal thiazide-sensitive NaCl cotransport. *J. Am. Soc. Nephrol.* **9:**819–826
2. Altschul, S.F., Madden, T., Schaffer, A.A., Zhang, J., Zhang, Z., Miller, W., Lipman, D.J. 1997. Gapped BLAST and PSI-BLAST: a new generation of protein database search programs. *Nucleic Acids Res.* **25:**3389–3402
3. Barry, E.L.R., Gesek, F.A., Kaplan, M.R., Hebert, S.C., Friedman, P.A. 1997. Expression of the sodium-chloride cotransporter in osteoblastlike cells: effects of thiazide diuretics. *Am. J. Physiol.* **272:**C109–C116
4. Chang, H., Tashiro, K., Hirai, M., Ikeda, K., Kurokawa, K., Fujita, T., 1996. Identification of a cDNA encoding a thiazide-sensitive sodium-chloride cotransporter from the human and its mRNA expression in various tissues. *Biochem. Biophys. Res. Comm.* **223:**324–328
5. Corcia, A., Armstrong, W.McD. 1983. KCl cotransport: a mechanism for basolateral chloride exit in Necturus gallbladder. *J. Membrane Biol.* **76:**173–182
6. Costanzo, L.S., Windhager, E.E. 1978. Calcium and sodium transport by distal convoluted tubule of the rat. *Am. J. Physiol.* **235:**F492–F506
7. Cremaschi, D., Hénin, S. 1975. Na^+ and Cl^- transepithelial routes in rabbit gallbladder. Tracer analysis of the transports. *Pfluegers Arch.* **361:**33–41
8. Cremaschi, D., Hénin, S., Ferroni, A. 1974. Intracellular electric potential in the epithelial cells of rabbit gallbladder. *Bioelectrochem. Bioenerg.* **1:**208–216
9. Cremaschi, D., Hénin, S., Meyer, G. 1979. Stimulation by HCO_3^- of Na^+ transport in rabbit gallbladder. *J. Membrane Biol.* **47:**145–170
10. Cremaschi, D., Meyer, G. 1982. Amiloride sensitive sodium channels in rabbit and guinea-pig gallbladder. *J. Physiol.* **326:**21–34
11. Cremaschi, D., Meyer, G., Bermano, S., Marcati, M. 1983. Different sodium chloride cotransport systems in the apical membrane of rabbit gallbladder epithelial cells. *J. Membrane Biol.* **73:**227–235
12. Cremaschi, D., Meyer, G., Bottà, G., Rossetti C. 1987. The nature of the neutral Na^+-Cl^- coupled entry at the apical membrane of rabbit gallbladder epithelium: II. Na^+-Cl^- symport is independent of K^+. *J. Membrane Biol.* **95:**219–228
13. Cremaschi, D., Meyer, G., Rossetti, C. 1983. Bicarbonate effects, electromotive forces and potassium effluxes in rabbit and guinea-pig gallbladder. *J. Physiol.* **335:**51–64
14. Cremaschi, D., Meyer, G., Rossetti, C., Bottà, G., Palestini, P. 1987. The nature of the neutral Na^+-Cl^- coupled entry at the apical membrane of the rabbit gallbladder epithelium: I. $Na^+/H^+,Cl^-/HCO_3^-$ double exchange and Na^+-Cl^- symport. *J. Membrane Biol.* **95:**209–218
15. Cremaschi, D., Porta, C. 1994. Hydrochlorothiazide enhances the apical Cl^- backflux in rabbit gallbladder epithelium: radiochemical analysis. *J. Membrane Biol.* **141:**29–42
16. Cremaschi, D., Porta, C., Bottà, G., Meyer, G. 1992. Nature of the neutral Na^+-Cl^- coupled entry at the apical membrane of rabbit gallbladder epithelium: IV. $Na^+/H^+,Cl^-/HCO_3^-$ double exchange, hydrochlorothiazide-sensitive Na^+-Cl^- symport and Na^+-K^+-$2Cl^-$ cotransport are all involved. *J. Membrane Biol.* **129:**221–235
17. Cremaschi, D., Porta, C., Riccardi, D., Bottà, G., Meyer, G. 1992. The three forms of NaCl neutral entry are all present in the apical membrane of rabbit gallbladder epithelium. *J. Gen. Physiol.* **100:**45–46*a*
18. Cremaschi, D., Vallin, P., Porta C. 1995. Hydrochlorothiazide action on the apical Cl^-, Ca^{2+} and K^+ conductances in rabbit gallbladder epithelium. Presence of an apamin-sensitive, Ca^{2+}-activated K^+ conductance. *J. Membrane Biol.* **147:**159–171
19. Duffey, M.E., Frizzell, R.A. 1984. Flounder urinary bladder.

Mechanism of inhibition by hydrochlorothiazide (HCTZ). *Fed. Proc.* **43:**932 (*Abstr.*)
20. Frizzell, R.A., Dugas, M.C., Schultz, S.G. 1975. Sodium chloride transport by rabbit gallbladder. Direct evidence for a coupled NaCl influx process. *J. Gen. Physiol.* **65:**769–795
21. Gamba, G., Miyanoshita, A., Lombardi, M., Lytton, J., Lee, W., Hediger, M.A., Hebert, S.C. 1994. Molecular cloning, primary structure, and characterization of two members of the mammalian electroneutral sodium-(potassium)-chloride cotransporter family expressed in kidney. *J. Biol. Chem.* **269:**17713–17722
22. Gamba, G., Saltzberg, S.N., Lombardi, M., Miyanoshita, A., Lytton, J., Hediger, M.A., Brenniger, M.B., Hebert, S.C. 1993. Primary structure and functional expression of a cDNA encoding the thiazide-sensitive, electroneutral sodium-chloride cotransporter. *Proc. Natl. Acad. Sci.* **90:**2749–2753
23. Hénin, S., Cremaschi, D. 1975. Transcellular ion route in rabbit gallbladder. Electric properties of the epithelial cells. *Pfluegers Arch.* **355:**125–139
24. Hoover, R.S., Mount, D.B., Gamba, G., Hebert, S.C. 1996. Characterization of an alternatively spliced isoform of the rat thiazide-sensitive Na-Cl cotransporter. *J. Am. Soc. Nephrol.* **7:**1281 (*Abstr.*)
25. Mastroianni, N., De Fusco, M, Zollo, M., Arrigo, G., Zuffardi, O., Bettinelli, A., Ballabio, A., Casari, G. 1996. Molecular cloning, expression pattern, and chromosomal localization of the human Na-Cl thiazide-sensitive cotransporter (SLC12A3). *Genomics* **35:**486–493
26. Meyer, G., Bottà, G., Rossetti, C., Cremaschi, D. 1990. The nature of the neutral Na^+-Cl^- coupled entry at the apical membrane of rabbit gallbladder epithelium: III. Analysis of transport on membrane vesicles. *J. Membrane Biol.* **118:**107–120
27. Meyer, G., Rossetti, C., Bottà, G., Cremaschi, D. 1985. Construction of K^+- and Na^+-sensitive theta microelectrodes with fine tips. An easy method with high yield. *Pfluegers Arch.* **404:**378–381
28. Mount, D.B., Delpire, E., Gamba, G., Hall, A.E., Poch, E., Hoover Jr, R.S., Hebert, S.C. 1998. The electroneutral cation-chloride cotransporters. *J. Exp. Biol.* **200:**2091–2102
29. Mount, D.B., Hoover, R.S., Hebert, S.C. 1997. The molecular physiology of electroneutral cation-chloride cotransport. *J. Membrane Biol.* **158:**177–186
30. Nellans, H.N., Frizzell, R.A., Schultz, S.G. 1973. Coupled sodium chloride influx across the brush border of rabbit ileum. *Am. J. Physiol.* **225:**467–475.
31. Reuss, L. 1983. Basolateral KCl cotransport in a NaCl-absorbing epithelium. *Nature* **305:**723–726
32. Reuss, L., Weinman, S.A., Grady, T.P. 1980. Intracellular K^+ activity and its relation to basolateral membrane ion transport in Necturus gallbladder epithelium. *J. Gen. Physiol.* **76:**33–52
33. Sambrook, J., Fritsch, E.F., Maniatis, T. 1989. Molecular Cloning. A Laboratory Manual, Cold Spring Harbor, New York
34. Schultz, S.G., Zalusky, R. 1964. Ion transport in isolated rabbit ileum: I. Short circuit current and Na fluxes. *J. Gen. Physiol.* **47:**567–584
35. Simon, D.B., Nelson-Williams, C., Bia, M.J., Ellison, D., Karet, F.E., Molina, A.M., Vaara, I., Iwata, F., Cushner, H.M., Koolen, M., Gainza, F.J., Gitelman, H.J., Lifton, R.P. 1996. Gitelman's variant of Bartter's syndrome, inherited hypokalaemic alkalosis, is caused by mutations in the thiazide-sensitive Na-Cl cotransporter. *Nat. Genet.* **12:**24–30
36. Stokes, J.B. 1984. Sodium chloride absorption in the urinary bladder of the winter flounder. A thiazide-sensitive electrically neutral transport system. *J. Clin. Inv.* **74:**7–16
37. Van Os, C.H., Slegers, J.F.G. 1975. The electrical potential profile of gallbladder epithelium. *J. Membrane Biol.* **24:**341–363
38. Velasquez, H. 1987. Thiazide diuretics. *Renal Physiol.* **10:**184–197
39. Velasquez, H., Good, D.W., Wright, F.S. 1984. Mutual dependence of sodium and chloride absorption by renal distal tubule. *Am. J. Physiol.* **247:**F904–F911